

Supplemental Materials

Table S1. Two-year mean and seasonal statistics of collocated SEVIRI and MODIS retrievals in rain-free, ice-free, smoke-free (AI < 0.1), $\tau > 3$, and overcast (LCF $\geq 95\%$) grid cells over the marine stratocumulus region. The τ means and r_e means (in micron) are listed. The values in brackets are statistics without filtering for LCF $\geq 95\%$ and $\tau > 3$, i.e., for the all-sky case.

	JJA	SON	DJF	MAM	Two-year
Stratocumulus (SEVIRI vs. MODIS)					
SEVIRI τ	10.2 (5.9)	10.3 (7.1)	9.9 (5.2)	9.9 (4.8)	10.2 (6.0)
MODIS 1.6 τ	11.3 (7.3)	11.3 (8.3)	10.8 (6.3)	10.8 (5.9)	11.1 (7.2)
SEVIRI r_e	8.8 (10.2)	10.2 (11.1)	11.6 (11.4)	10.5 (10.7)	10.1 (10.9)
MODIS 1.6 r_e	10.3 (12.6)	11.5 (12.9)	12.2 (13.4)	11.4 (13.2)	11.3 (13.0)
MODIS 2.1 r_e	11.1 (13.8)	11.9 (13.3)	12.3 (13.4)	11.6 (13.6)	11.7 (13.5)
MODIS 3.7 r_e	11.5 (12.6)	11.7 (12.5)	11.6 (11.9)	11.2 (11.8)	11.6 (12.2)
Correl. τ 1.6	0.96 (0.93)	0.97 (0.96)	0.96 (0.95)	0.96 (0.94)	0.96 (0.95)
Correl. r_e 1.6	0.93 (0.73)	0.90 (0.76)	0.92 (0.60)	0.92 (0.62)	0.92 (0.70)
Correl. r_e 2.1	0.90 (0.77)	0.90 (0.77)	0.91 (0.62)	0.92 (0.67)	0.89 (0.72)
Correl. r_e 3.7	0.86 (0.81)	0.78 (0.76)	0.87 (0.64)	0.87 (0.64)	0.80 (0.74)

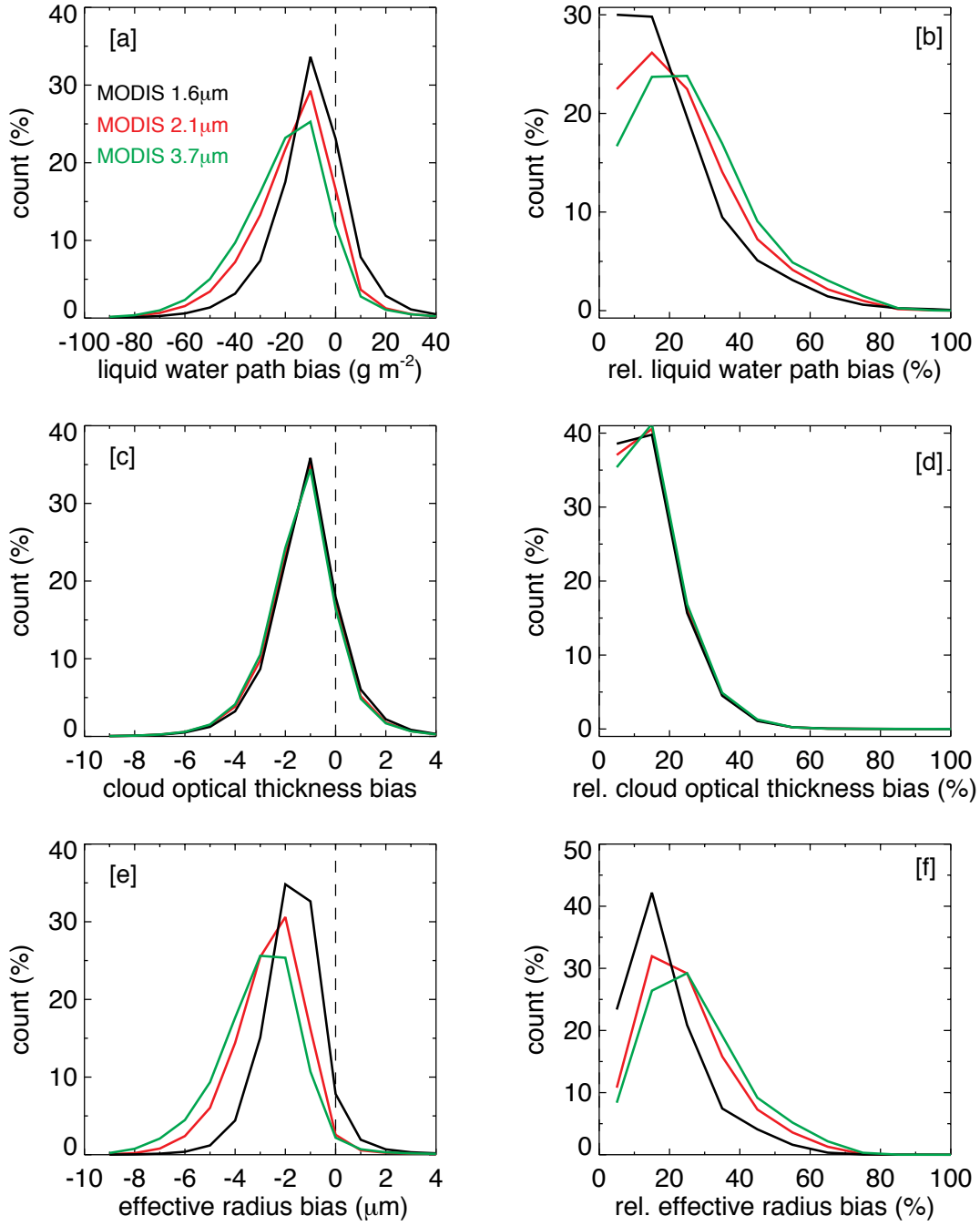
Discussion: Frequency histograms of SEVIRI – MODIS LWP, τ , and r_e difference, as well as, the differences relative to MODIS LWP, τ , and r_e for the overcast condition aggregated during JAS 2011 and JAS 2012 are shown in Fig. S1. The histogram of SEVIRI – MODIS τ differences revealed that the peak of the distribution is off zero with ~35 % of the data falling into the -1 bin. Only ~17 % of data showed mean zero difference, while ~23 % of data showed a difference of -2. The SEVIRI τ relative to MODIS τ was within 10 % for 36 % of the data, within 20 % for 80 % of the data, and within 30 % for 95 % of the retrievals. Overall, SEVIRI τ appeared to be low by ~1 compared to MODIS τ .

SEVIRI r_e retrieved in the 1.6- μm channel was compared with MODIS r_e values retrieved in three water absorbing channels at 1.6-, 2.1-, and 3.7- μm . Compared to the 1.6- μm MODIS r_e , ~70 % of SEVIRI r_e have a mean difference of -1.5 μm . Compared to the 2.1- and 3.7- μm MODIS r_e , the difference histograms indicate larger

differences: $\sim 55\%$ and $\sim 50\%$ of SEVIRI r_e have a difference of $-2.5\ \mu\text{m}$, respectively. Although SEVIRI r_e are biased low compared to all three MODIS r_e , the $\sim 1\ \mu\text{m}$ additional low bias relative to the 2.1- and 3.7- μm r_e likely indicates much smaller smoke-induced retrieval artifacts in these two channels. In general, the r_e retrievals from SEVIRI tend to be lower than corresponding retrievals from the three MODIS channels, with SEVIRI having about 1.5 μm to 2.5 μm lower r_e values.

The SEVIRI minus MODIS LWP distributions peak at about $-10\ \text{g m}^{-2}$ irrespective of the MODIS channel used for the retrieval. The differences between MODIS 1.6- μm and SEVIRI retrievals are within 10 % for about 30 % of SEVIRI pixels, within 20 % for about 60 % of the SEVIRI pixels, and within 30 % for about 80 % of the SEVIRI pixels. However, differences between SEVIRI and MODIS 2.1- μm and 3.7- μm channel retrievals are larger, with relative differences being smaller than 10 % for about 22 % of the SEVIRI pixels against MODIS 2.1- μm and for about 16 % of the SEVIRI pixels against MODIS 3.7- μm values.

The frequency histograms of SEVIRI – MODIS LWP, τ , and r_e differences, as well as the difference with respect to different MODIS channels for the 2-year aggregate are shown in Fig. S3 (all-sky case) and Fig. S4 (overcast case). The peak of the LWP absolute/relative difference distribution is centred on zero, although the distribution is negatively skewed. Interestingly, in the all-sky case $\sim 40\%$ of the data have shown negligible difference (zero LWP bias bin), whereas, only about 30 % of the data have shown a negligible difference in the overcast case. About 20–30 % of the data have fallen into the LWP difference bin of $-10\ \text{g m}^{-2}$ in either cases. In the overcast case, $\sim 40\%$ of the data have shown a relative LWP difference $< 10\%$ and $\sim 90\%$ of the data have shown a relative LWP difference $< 30\%$; however, for the all-sky case, only about 25 % and 60 % of the data have shown relative LWP differences $< 10\%$ and $< 30\%$. Respectively, about 48 %, 84 %, 95 % of the observations show relative τ differences within 10 %, 20 %, and 30 % in the overcast case. Similarly, about 90 % of the observations show relative r_e differences within 30 % in the overcast case. Histograms of both τ and r_e differences reveal that the distribution is off centered. Histograms of τ differences reveal a narrow distribution which peaks at -1 especially in the overcast case; however in the all-sky case a broader peak is noticed between -1 and 0. Histograms of r_e differences reveal wider distributions (especially when compared against the 2.1- and 3.7- μm channels), which peak at -1 μm in the overcast case; however, in the all-sky case a broader peak is noticed between -2 μm and -1 μm .



50

Figure S1. Histogram of SEVIRI – MODIS liquid water path differences (a), cloud optical thickness differences (c), and droplet effective radius differences (e), as well as, histogram of SEVIRI – MODIS LWP, τ , r_e differences relative to MODIS LWP (b), τ (d), and r_e (f) for JAS 2011 and JAS 2012 for overcast ($\text{LCF} \geq 95\%$ and $\tau > 3$) rain- and ice-free conditions.

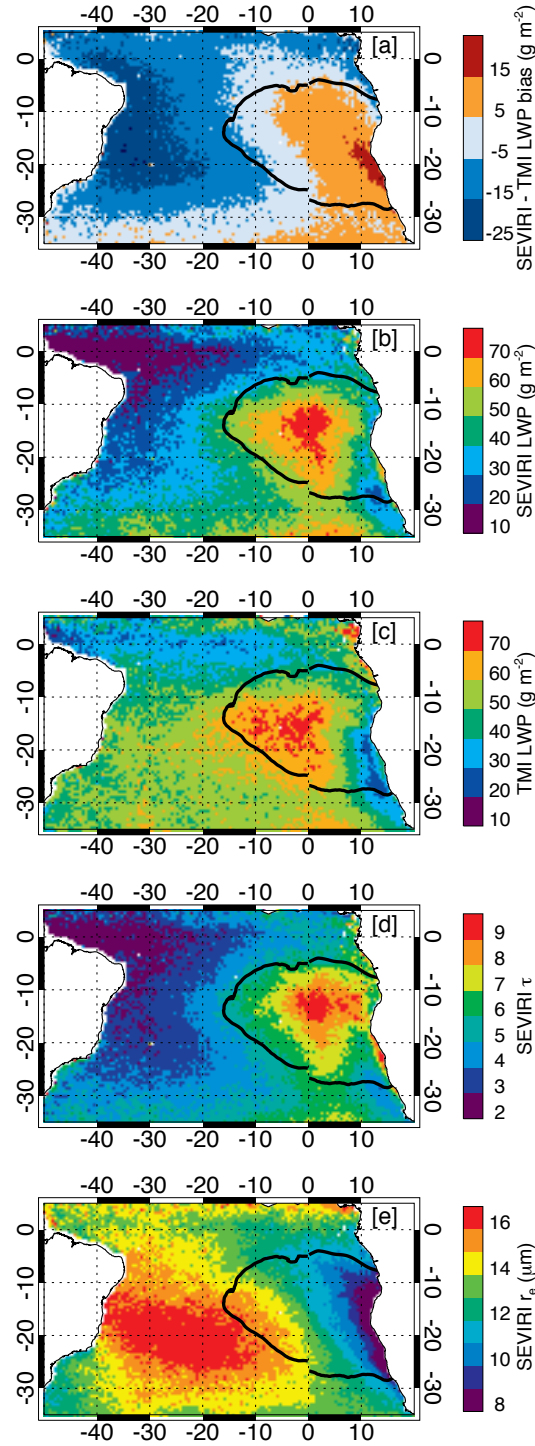
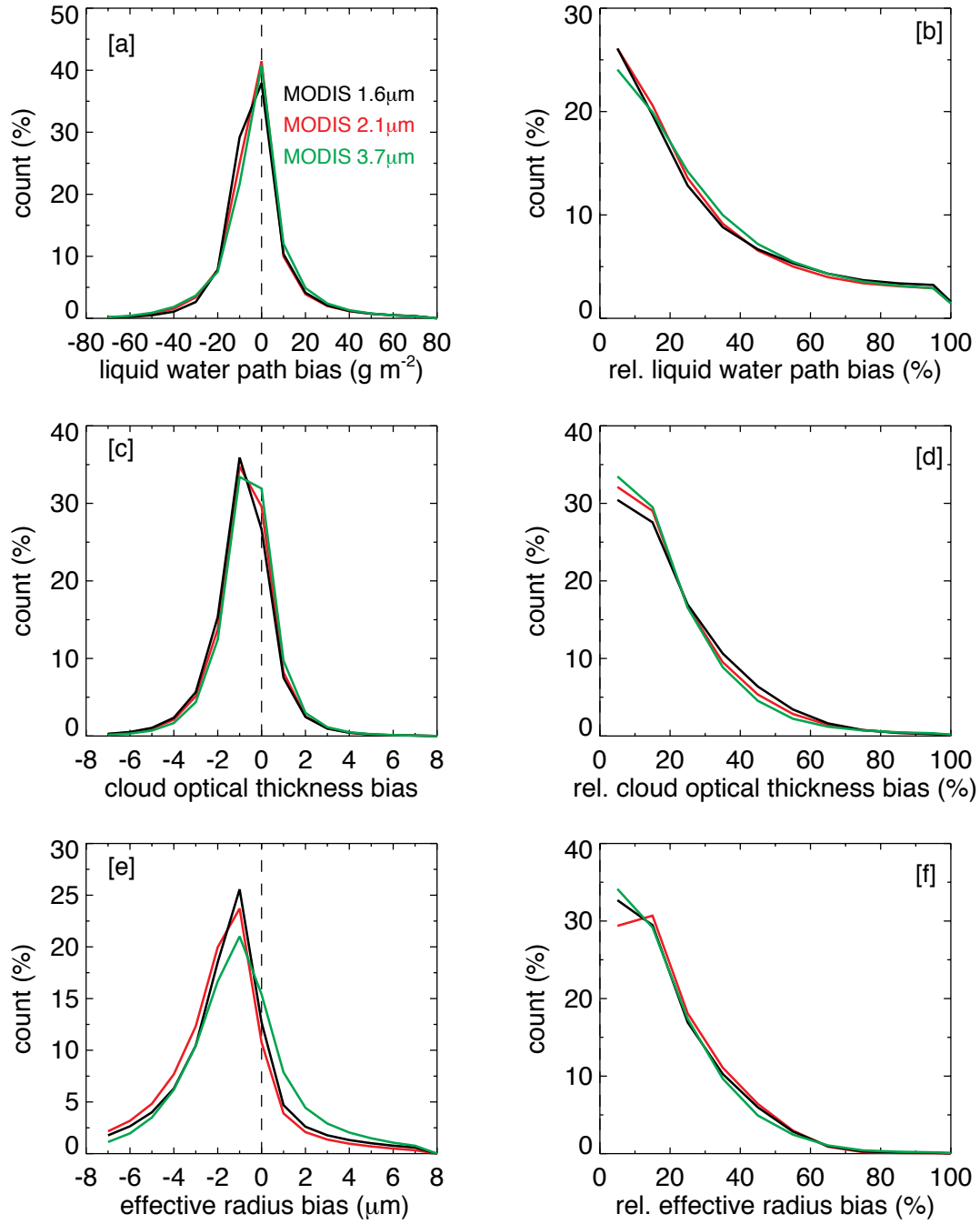
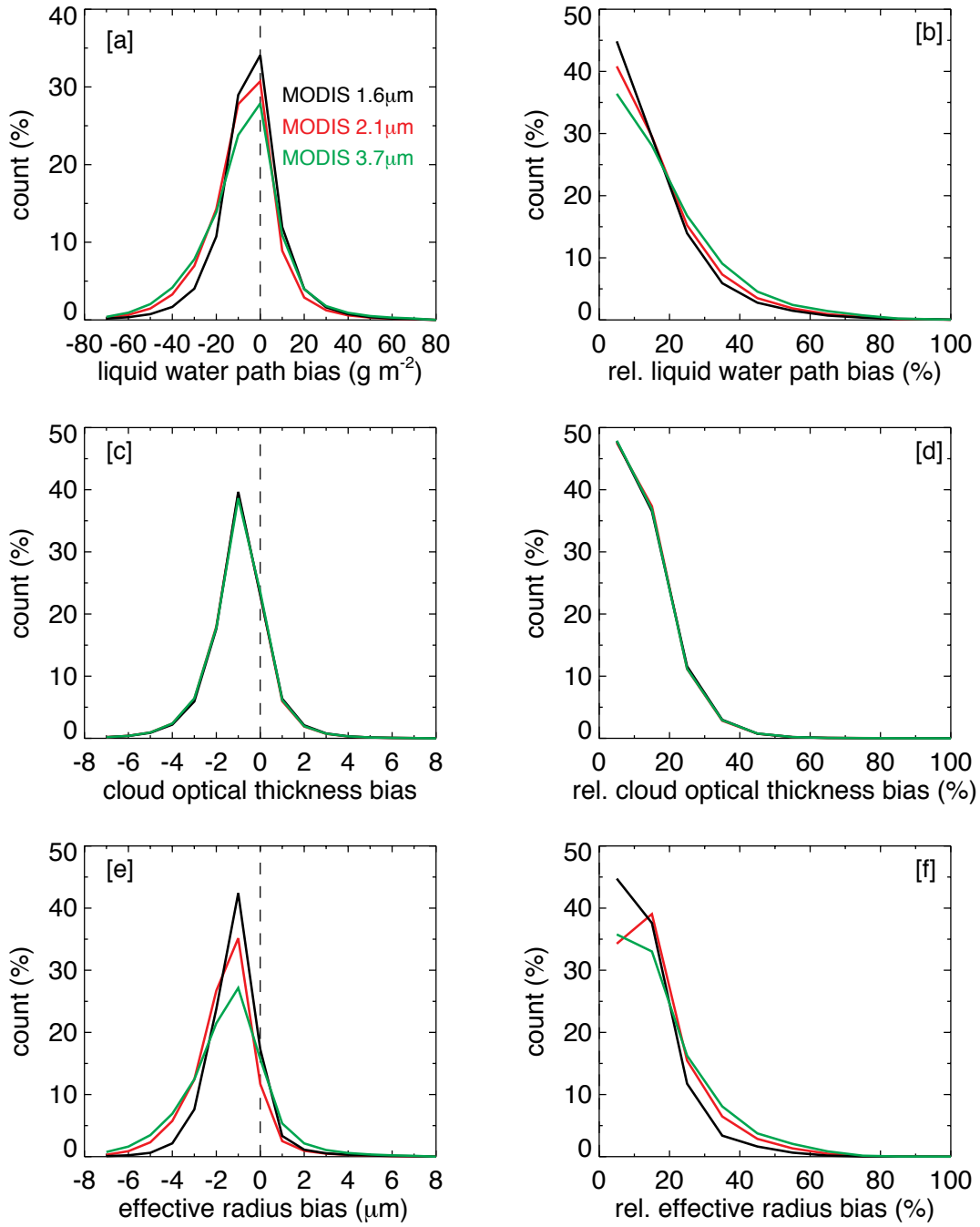


Figure S2. Two-year mean map of (a) SEVIRI minus TMI LWP difference, (b) SEVIRI LWP, (c) TMI LWP, (d) SEVIRI τ , (e) SEVIRI 1.6- μm r_e , for the all-sky case. The solid black contour denotes the identified Sc region. Rain-, ice-, and aerosol-free conditions were applied.



65

Figure S3. Histogram of SEVIRI – MODIS liquid water path differences (a), cloud optical thickness differences (c), and droplet effective radius differences (e), as well as, histogram of SEVIRI – MODIS LWP, τ , r_e differences relative to MODIS LWP (b), τ (d), and r_e (f) for December 2010 to November 2012 for the all-sky case with rain- and ice-free conditions.



70

75

Figure S4. Histogram of SEVIRI – MODIS liquid water path differences (a), cloud optical thickness differences (c), and droplet effective radius differences (e), as well as, histogram of SEVIRI – MODIS LWP, τ , r_e differences relative to MODIS LWP (b), τ (d), and r_e (f) for December 2010 to November 2012 for the overcast case ($\text{LCF} \geq 95\%$ and $\tau > 3$) in rain- and ice-free conditions.

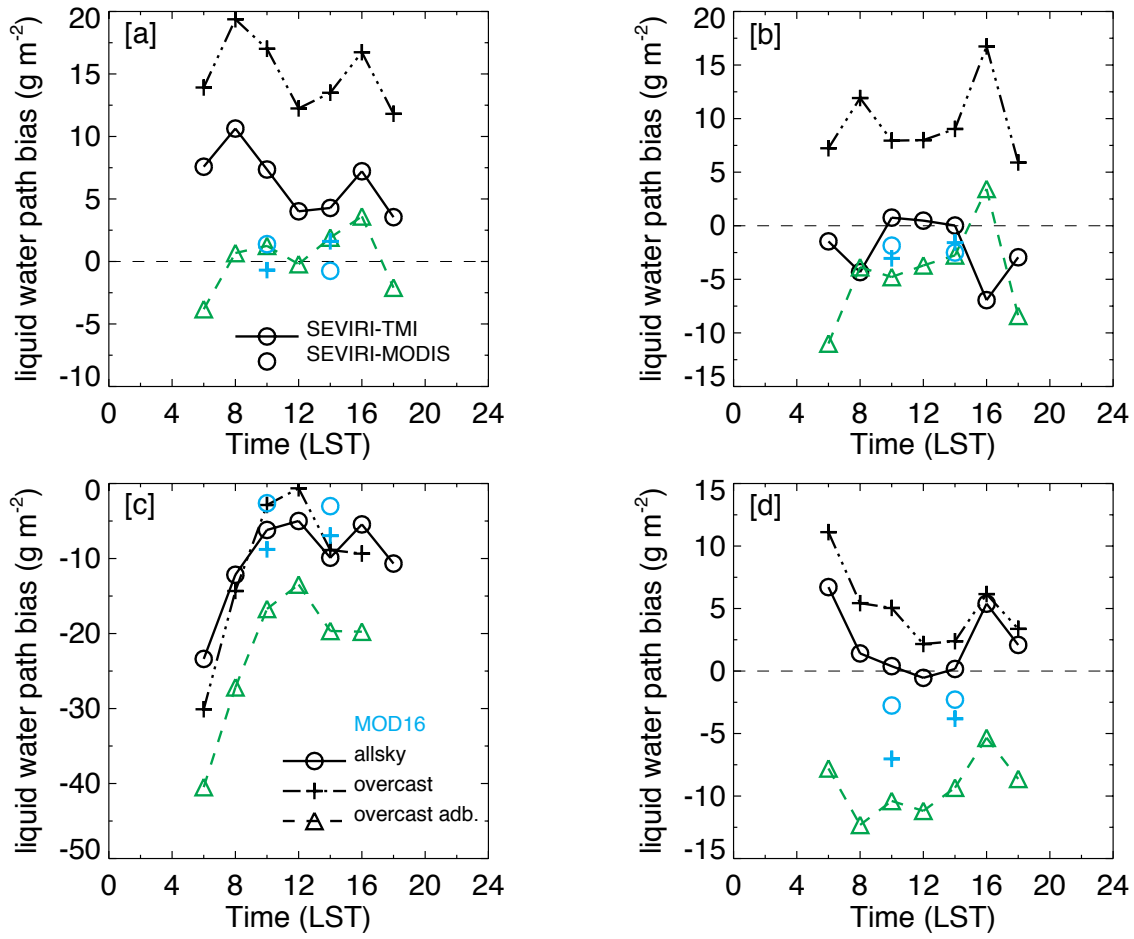
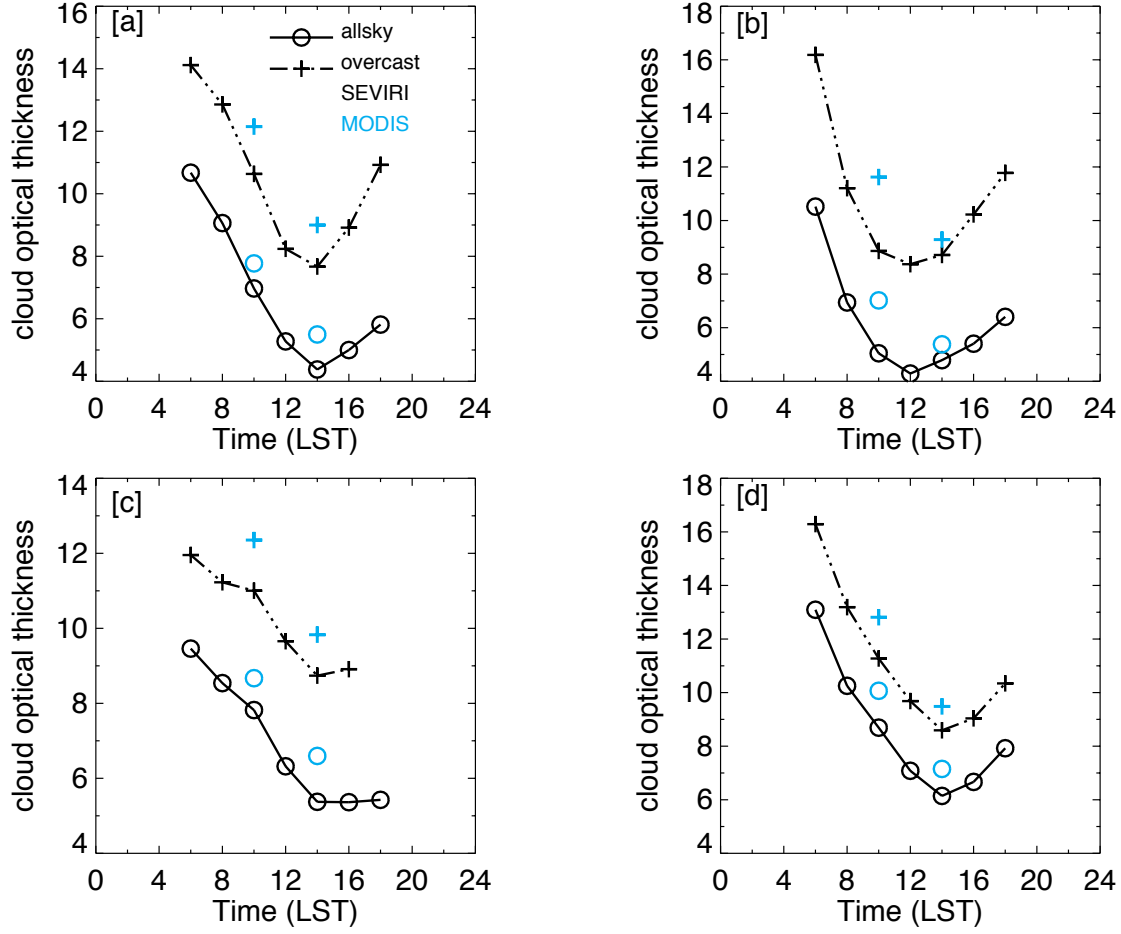


Figure S5. Seasonal mean diurnal cycle of SEVIRI LWP bias compared to TMI as well as Terra and Aqua MODIS, over the Sc region, both for all-sky and overcast-cases ($\text{LCF} \geq 95\%$ and $\tau > 3$): (a) DJF, (b) MAM, (c) JJA, and (d) SON of the study period. Rain-, ice-, and smoke-free conditions were applied.



95

100

Figure S6. Seasonal mean diurnal cycle of SEVIRI and Terra and Aqua MODIS cloud optical thicknesses over the Sc region, both for all-sky and overcast-cases ($\text{LCF} \geq 95\%$ and $\tau > 3$): (a) DJF, (b) MAM, (c) JJA, and (d) SON of the study period.

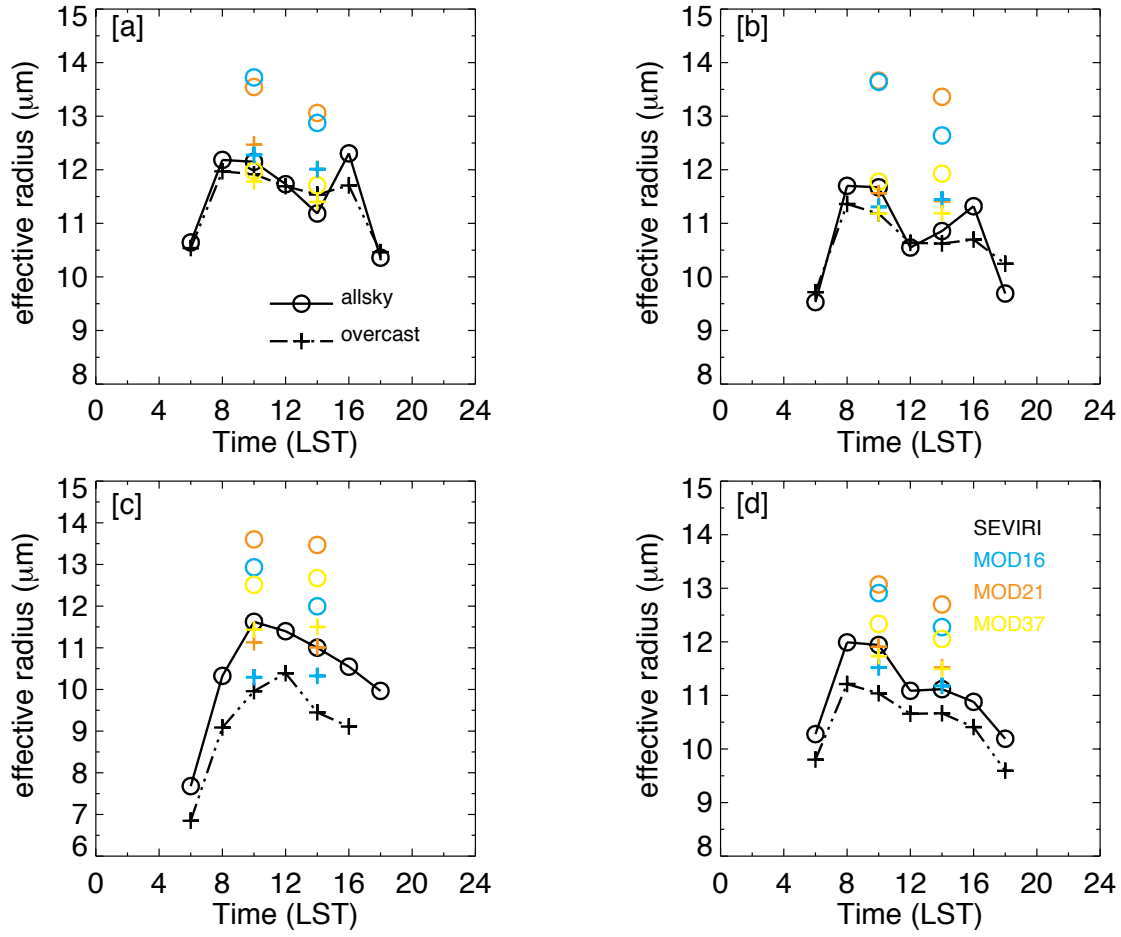


Figure S7. Seasonal mean diurnal cycle of SEVIRI and Terra and Aqua MODIS cloud droplet effective radius over the Sc region, both for all-sky and overcast-cases (LCF $\geq 95\%$ and $\tau > 3$): (a) DJF, (b) MAM, (c) JJA, and (d) SON of the study period.

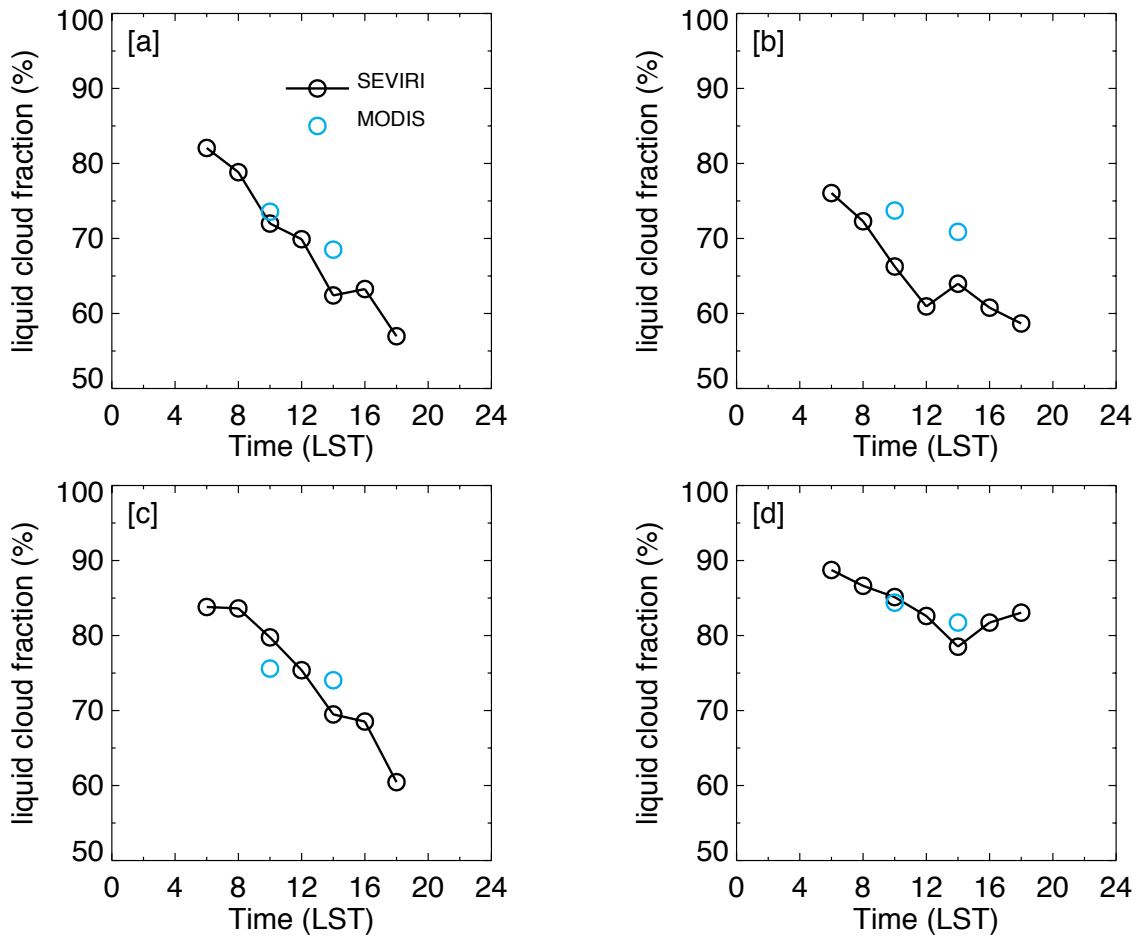


Figure S8. Seasonal mean diurnal cycle of SEVIRI and Terra and Aqua MODIS liquid cloud fraction over the Sc region, for all-sky case: (a) DJF, (b) MAM, (c) JJA, and (d) SON of the study period.